Effect of a part-hour shading methodology on the sensitivity of shading calculations to horizon uncertainty

Joseph Ranalli and David J. Starling

**Abstract**

A previous study investigated how horizon measurement uncertainty leads to errors in annual irradiance calculations. Those results were based upon determining shading for whole hour periods by testing whether the mid-hour point fell below the horizon. In this study, we test an alternate approach that considers fractional shading during each hourly window. We find only very slight changes in the P90 sensitivity of irradiance to horizon measurement errors. In the previous study, we observed that approaches using whole-hour shading resulted in a maximum sensitivity that increased as smaller position increments were considered for the horizon measurement error. Here, we observe that part-hour shading is less sensitive to the magnitude of these errors, especially with regard to horizon azimuthal measurement. Additionally, we find that the maximum sensitivity is reduced when considering these smaller position increments. The decision to adopt a part-hour shading methodology requires balancing the relatively minor benefits against the additional computational complexity required for the approach.

**Introduction**

Solar energy is an important component of increased worldwide renewable energy deployment. Like most renewable energy technologies, solar energy's financial case is based upon lifecycle analysis. As compared to traditional energy systems, high initial costs are offset by low operating costs, resulting in an economic payback that may be realized after a few years. These high upfront costs motivate those with vested stakes in solar energy systems to plan their installation in a way that minimizes risk and uncertainty to the highest extent possible (Vignola et al., 2012).

A number of factors affect the performance of solar energy installations. Uncertainty in each of these factors affects the overall system uncertainty. A detailed estimation of these uncertainties was conducted by Thevenard and Pelland (Thevenard and Pelland, 2013), who estimate an overall uncertainty of around 8% from all contributing factors. Better understanding of the sources of uncertainty in solar energy calculations could help reduce financial risk and promote broader adoption.

A previous study by the authors has attempted to provide a more detailed understanding of the errors in annual solar energy system performance stemming from uncertainties in the measurement of a horizon that propagate through shading calculations (Ranalli et al., 2017). These errors were evaluated by simulating the uncertainty in the measurement of the position of obstacles on the horizon and investigating the impact that this had on the annual irradiance calculations. One limitation in the previous work was that shading was considered to be binary for each hour (shaded or unshaded) based solely on the sun's mid-hour position. This made estimation of the maximum sensitivity to horizon position errors difficult, as small changes in obstacle position resulted in step changes in the power produced, due to the hourly clustering of sun positions from the collector's perspective.

**Methodology**

In this study, we have adopted a partial-hour shading approach that allows us to examine any limitations in the previous study caused by the binary shading approach. The calculation methodology used exactly matched that of Ranalli et al. (Ranalli et al., 2017), with only the binary vs. part-hour shading calculation method changed. The Software Development Kit for System Advisor Model (SAM) (Blair et al., 2014) was used to perform solar irradiance calculations, using the 2013 version of the PVSAMV1 module. By default, SAM used the Perez model (Perez et al., 1990) to compute plane-of-array irradiance based on input TMY3 files from the National Solar Radiation Database (Wilcox, 2012).

Shading was simulated by considering rectangular obstacles with variable height, width and azimuthal center. Sensitivities were calculated by observing changes in predicted annual irradiance per unit shift in obstacle position angle. We defined the sensitivity as the ratio between the change in normalized shaded annual irradiance, $dG_{sh}^{*}$, to the change in angular position, $d\varphi$, as shown in Eq. 1. In the prior study, it was determined that it is difficult to assign a single value to sensitivity, as it was found to depend on the absolute value of obstacle position parameters. Maximum sensitivities were also impossible to characterize as mentioned previously, due to the clustering of hourly sun positions. Thus, in the previous study, a representative P90 sensitivity was computed by identifying the 90$^{th}$ percentile value of sensitivity across all obstacle conditions computed. This achieved a linear measure of sensitivity that did not depend on the magnitude of the obstacle shift considered (Ranalli et al., 2017). In this study, along with the P90 value, we will also report the maximum sensitivity observed considering all obstacle conditions, to demonstrate the influence of using the part-hour shading approach.

Eq 1 $$sensitivity = \frac{dG_{sh}^{*}}{d\varphi}$$

Shading was determined considering separate beam and diffuse shade factors, $f_b$ and $f_d$ (Drif et al., 2008). The diffuse shade factor is defined as a view factor correction between the collector and the sky dome (Quaschning and Hanitsch, 1995). Since this diffuse shading view factor is geometric in nature (i.e. is computed only based on the stationary sky dome), it is independent of the sun's position and experiences no changes between whole-hour and part-hour shading approaches. Thus the same sensitivities of diffuse shade factor to horizon measurement error as in the previous study can be expected to hold (see Table 1).

**Table 1 - P90 diffuse shade factor sensitivities. Reproduced from (Ranalli et al., 2017).**

| Parameter | P90 sensitivity |
|---|---|
| Center | 0.5% |
| Width | 1.0% |
| Height | 0.4% |

In order to compute the beam shading factor using a part-hour approach, each hour was divided into 30 timespans (corresponding to 2 minutes each), centered evenly about the mid-hour point. Sun positions during these sub-hour timespans were computed using the same methodology as the underlying SAM package (Gilman, 2014). A mid-point of each sub-hour timespan was used to determine whether the timespan in question was shaded. Hourly beam shade factors, now taking fractional values, were computed for each full hour in the TMY3 weather file, by taking the ratio of the number of shaded sub-hour points to the total number of sub-hour points (usually 30, but fewer if sunrise or sunset occurred during a given hour). An example is shown in Fig. 1. The fractional beam shading factor is used by SAM to linearly scale the beam portion of the irradiance only. Because the prior study demonstrated that the results did not significantly depend on the TMY3 file chosen, in this case, we will consider only a single TMY3 site: Wilkes-Barre, PA.

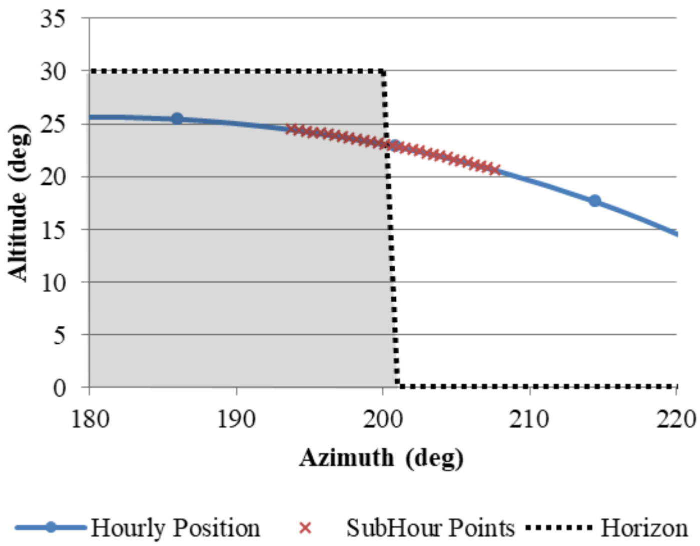


**Fig. 1 - Depiction of the part-hour points used to evaluate shading. Fourteen of the 30 part-hour points are currently shaded, resulting in a beam shading factor of $f_b = 0.47$.**

As in the prior study, we created a set of simulated flat-top obstacles with varying azimuthal width angle ($\varphi_w$), overall obstacle angular height (in altitude, $\varphi_h$) and central azimuth angles ($\varphi_c$). The ranges of conditions tested for each of these parameters are given in Table 2. Sensitivity was measured as the change in shade factor relative to each of these variables. A composite sensitivity was also calculated according to a standard propagation of uncertainty as in Eq. 2. The standard deviations ($\sigma_{alt}, \sigma_{az}$) represent the uncertainty associated with the horizon measurement device along each angular position. As in the previous study, a smartphone-based horizon measurement sensor was used as a reference device with uncertainty of 5° standard deviation in azimuth and 0.5° standard deviation in altitude (Ranalli, 2015).

Eq 2. $$\sigma = \sqrt{\left(\frac{df}{d\varphi_h}\right)^2 {\sigma_{alt}}^2 + \left[\left(\frac{df}{d\varphi_c}\right)^2 + \left(\frac{df}{d\varphi_w}\right)^2\right] {\sigma_{az}}^2}$$

**Table 2 - Obstacle limits used to produce the data**

| Parameter | Limits | Increment |
|---|---|---|
| Center | -180° to +180° | 10° |
| Width | 0-270° | 10° |
| Height | 0-90° | 10° |

## Results

We calculated the sensitivity of irradiance to each horizon obstacle position variable for the Wilkes-Barre, PA TMY3 dataset, and present the results in Fig. 2. This figure looks very similar to its counterpart for whole-hour shading [see (Ranalli et al., 2017)], with the exception that it appears to be smoothed.

This smoothing is reasonable, given that the part-hour shading methodology more finely accounts for changes in obstacle position than the whole-hour case. However, when calculating P90 sensitivities over the full range of obstacle positions tested, we observe essentially no change in sensitivity to horizon position as shown in Table 3. This can be attributed to the fact that we are considering relatively large (10°) increments in the obstacle position, and looking at a P90 value for sensitivity. As demonstrated in the previous study, considering P90 sensitivity eliminates (or at least reduces) the dependence of computed sensitivity on the magnitude of the obstacle shift.

**Table 3 - P90 beam shade factor sensitivities compared for the two shading methodologies.**

| Parameter | Whole Hour P90 | Part Hour P90 |
|---|---:|---:|
| Center | 0.5% | 0.6% |
| Width | 1.2% | 1.2% |
| Height | 0.4% | 0.4% |

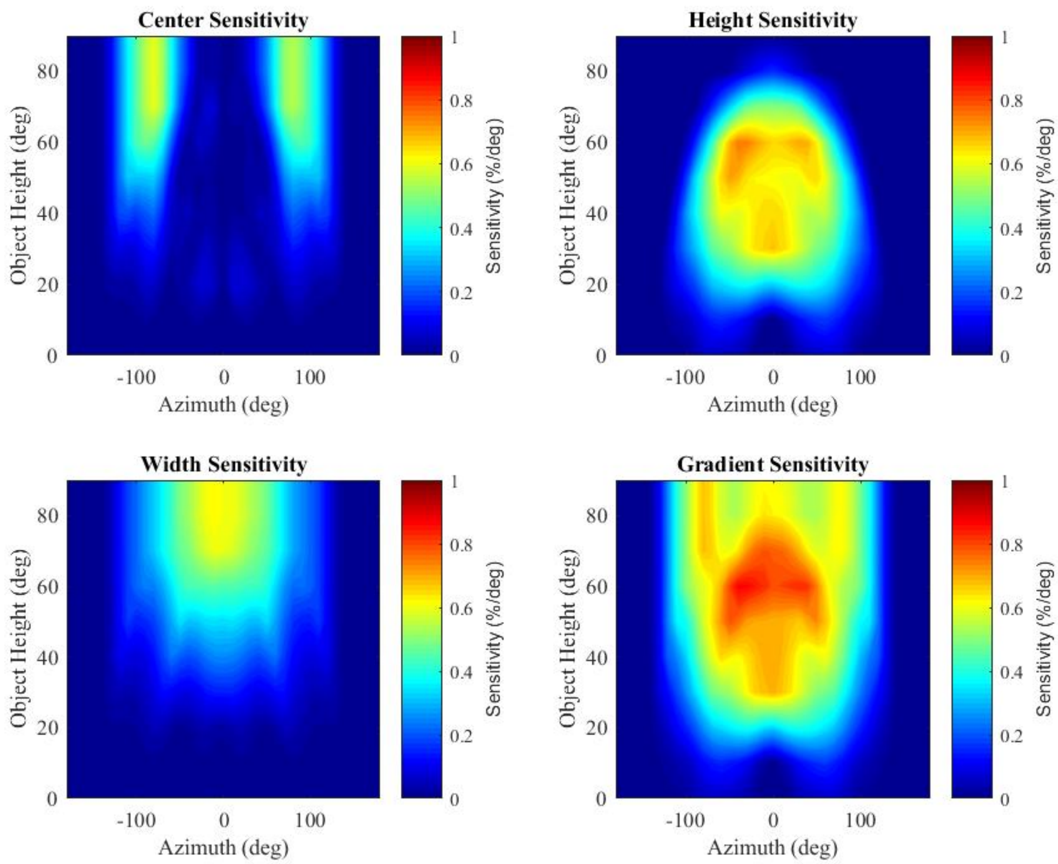


**Fig. 2- Sensitivity of irradiance to each horizon position variable.**

To better understand the differences that whole-hour and part-hour shading might exhibit in terms of sensitivity, we computed the maximum sensitivities observed over the full range of conditions tested. We did so for a multiple object position increments for each position variable, from 1° up to 20°, with results shown in Fig. 3. As is evident, the sensitivity for whole-hour shading is high for smaller object shifts, while part-hour shading is relatively independent of object shift magnitude. This is consistent with the results of the previous study, which indicated that small changes in the object position can cause large changes in the output, because of the clumping of hourly sun points. The independence of part-hour shading to shift increment is extremely evident for the center and width sensitivities, where the maximum sensitivity is reduced across the board and substantially so for small shifts of the obstacle.

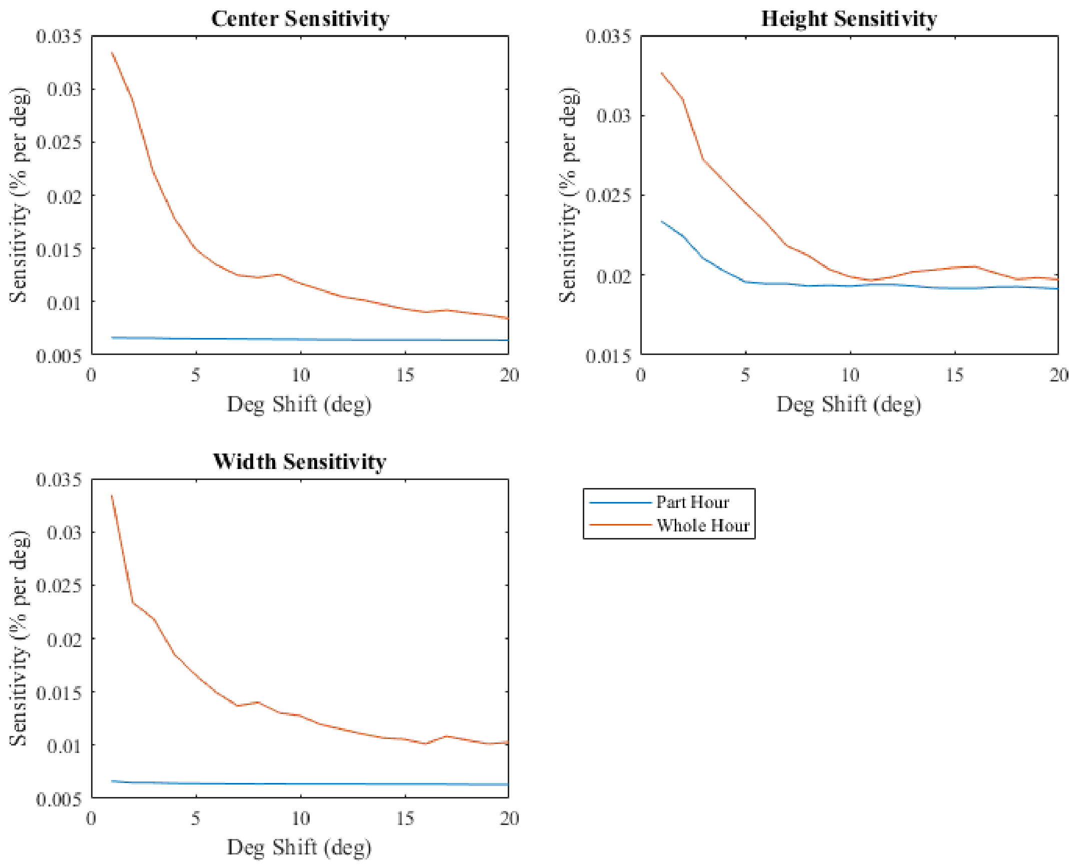


**Fig. 3 – Maximum sensitivity relative to the position variable increment used.**

## Discussion and Conclusions

Essentially no changes were observed between the part-hour and whole-hour approaches when considering P90 sensitivities. We interpret this as a result of the fact that using P90 eliminates rare, exaggerated maximum sensitivity values caused in the whole-hour case by clustering of the hourly sun positions. That is, P90 is already a linear representative measure for sensitivity that is independent of the absolute magnitude of the obstacle error considered and use of P90 allows sensitivity to be represented by a single value, as in the previous study, regardless of whether a part-hour or whole-hour shading approach is chosen. When considering maximum sensitivity, we observe that as we reduce the obstacle shift magnitude, whole-hour shading can be very sensitive to errors in the obstacle position. Part hour shading essentially eliminates this effect, rendering maximum sensitivity a second possible linear measure of the sensitivity. In either case, it is important to remember that these maximum sensitivity values occur due to interaction between whole-hour shading calculation and the clustered hourly sun positions; conditions which occur only for obstacles with very specific size/position characteristics.

As we observed no change of the P90 sensitivity between the previous and present studies, the recommended P90 sensitivity based on the sample measurement device uncertainties (5° standard deviation in azimuth, 0.5° standard deviation in altitude) remains at around 3%. We do however observe that when considering the rare maximum sensitivity cases that fall above the P90 window, utilizing a part-hour shading methodology limits the sensitivity of the calculations, particularly when considering position errors in azimuth. This small benefit comes at the non-trivial computational expense of computing additional sun positions, and testing each for shading (around 30x increased computational load for the shading portion in this case).

We conclude that the value of utilizing part-hour shading calculations lies in smoothing the sensitivity as a function of obstacle base position and limiting the maximum sensitivity that could be observed for a given obstacle shape/size. This is true for all of the obstacle position variables, but larger benefits are observed in the case of azimuthal position errors (obstacle center and width), as opposed to obstacle height. The impetus to perform these additional calculations should be weighed against the additional computational complexity. In general the shading calculations are not the dominant computational load, relative to the plane-of-array irradiance and PV system simulation. Overall, adopting a part-hour shading calculation methodology offers the opportunity to limit peak shading sensitivity.

**Acknowledgements**

The authors would like to acknowledge the contribution of students Mauro Notaro and Robert Vitagliano to the original research effort that this note extends.

**References**

Blair, N., Dobos, A.P., Freeman, J., Neises, T., Wagner, M., Ferguson, T., Gilman, P., Janzou, S., 2014. System Advisor Model, SAM 2014.1.14: General Description. National Renewable Energy Laboratory.

Drif, M., Pérez, P.J., Aguilera, J., Aguilar, J.D., 2008. A new estimation method of irradiance on a partially shaded PV generator in grid-connected photovoltaic systems. Renew. Energy 33, 2048–2056. https://doi.org/10.1016/j.renene.2007.12.010

Gilman, P., 2014. SAM Photovoltaic Model Technical Reference [WWW Document]. URL https://sam.nrel.gov/reference (accessed 10.14.14).

Perez, R., Ineichen, P., Seals, R., Michalsky, J., Stewart, R., 1990. Modeling daylight availability and irradiance components from direct and global irradiance. Sol. Energy 44, 271–289. https://doi.org/10.1016/0038-092X(90)90055-H

Quaschning, V., Hanitsch, R., 1995. Shade Calculations in Photovoltaic Systems. Presented at the ISES Solar World Conference, Zimbabwe.

Ranalli, J.A., 2015. Solar Survey: Development and validation of a smartphone-based solar site assessment tool. Sol. Energy 122, 1199–1213. https://doi.org/10.1016/j.solener.2015.10.039

Ranalli, J., Vitagliano, R., Notaro, M., Starling, D.J., 2017. Sensitivity of shading calculations to horizon uncertainty. Sol. Energy 144, 399–410. https://doi.org/10.1016/j.solener.2017.01.017

Thevenard, D., Pelland, S., 2013. Estimating the uncertainty in long-term photovoltaic yield predictions. Sol. Energy 91, 432–445. https://doi.org/10.1016/j.solener.2011.05.006

Vignola, F., Grover, C., Lemon, N., McMahan, A., 2012. Building a bankable solar radiation dataset. Sol. Energy 86, 2218–2229. https://doi.org/10.1016/j.solener.2012.05.013

Wilcox, S., 2012. National Solar Radiation Database 1991-2010 Update: User's Manual (No. NREL/TP-5500-54824). National Renewable Energy Laboratory.